Thermal Modulation Effects on Thermosolutal Convection in a Vertical Bridgman Cavity

E. A. Semma[1], M. El Ganaoui[2], V. Timchenko[3] and E. Leonardi[3]

Abstract: The effects of oscillatory heating on thermosolutal convection in a cavity heated from below are investigated and discussed. The transient Navier–Stokes equations coupled with heat and mass balances are solved numerically by using a control-volume technique. It is assumed that the interface moves with constant growth velocity. The results show the presence of multiple solutions in response to simultaneous vertical temperature and species concentration gradients applied to the system. In particular, two critical frequencies are identified, one corresponding to low values of the buoyancy ratio N ($N \sim 1$), accompanied with a decrease of flow intensity reaching a minimal value, the other occurring at higher value of N ($N \sim 50$), accompanied with flow intensity increase reaching a maximal value.

Keywords: Thermosolutal convection; thermal modulation; Bridgman cavity; finite volumes.

1 Nomenclature

C	dimensionless concentration
D	mass diffusivity
g	gravitational acceleration
H	height of the enclosure
k	thermal conductivity
Le	Lewis number, $= \alpha / D$
N	buoyancy ratio, $= \beta_C \Delta C' / \beta_T \Delta T'$
Nu	Nusselt number, see Eq (8)

---

[1] University of Hassan 1er, LM laboratory, Faculté des Sciences et Techniques de settat, B.P. 577, Settat, Morocco. Correspondence author: semmaalam@yahoo.fr

[2] University of Limoges, SPCTS laboratory, UMR 6638 CNRS, Faculty of Sciences and Technology 123, Albert Thomas 87060, Limoges, France.

[3] The University of New South Wales, Sydney, NSW 2052, Australia.

Pr   Prandtl number, $=\nu/\alpha$
Pe   Peclet number
Ra   thermal Rayleigh number, $=g\beta_T\Delta T'H^3/\upsilon\alpha$
Sh   Sherwood number, see Eq (8)
t   dimensionless time
T   dimensionless temperature
x,y   dimensionless coordinate system
u,v   dimensionless velocity terms

Greek symbol

α thermal diffusivity
β expansion coefficient
ν kinematic viscosity of fluid
ρ density of fluid
ψ dimensionless stream function

Subscript

c   critical
C   cold
H   hot
max   maximum
S   solutal
T   temperature
0   reference

Superscript

$'$ dimensional variable

2   Introduction

With very few exceptions, the solid materials we use (metallic alloys, glasses, ceramics, plastics, etc.) have all undergone a change from the liquid state to the

solid state. This transition affects the properties of the material: for instance, its microstructure (with or without grains), or its composition (with or without segregation). This depends on many parameters, such as the physical properties (very different in metals, glasses, or plastics) and the solidification system (crucible, cooling rate, pulling rate, an external action on the hydrodynamics of the fluid phase, etc.). Superimposed on such considerations is the way in which these effects influence the instantaneous shape of the interface (in general unstable) and the related phenomenon of solute absorption or rejection. This is indeed one of the major present scientific challenges for obtaining materials with desired properties and high performances (for a review the reader may consider El Ganaoui et al., 2007).

Directional solidification (Bridgman, Floating zone, ..) is one of the most used techniques of crystal growth because it permits processes with well-defined external controlling parameters [El Ganaoui 2002]. In order to investigate flow instabilities for Bridgman configurations, under full or low gravity conditions, fluid phase models in 2D configurations have been largely used by numerous authors [Crespo del Arco *et al.* 1989, Pulicani *et al.* 1990, Larroudé *et al.* 1994, El Ganaoui and Bontoux 1998, El Ganaoui et al 1999, Semma *et al.* 2003, Kaenton *et al.* 2004]. The control of such process is by the heating profile and the pulling velocity [Benielli et al 2001, Prud'homme & El Ganaoui 2006]. Flow and thresholds of unsteadiness may be further enhanced when thermal boundary conditions varying with time are considered. Such situations are encountered often, for instance, in periodically energized electronic components, solar energy collectors, and storage in ambient conditions, which induce unsteady heat generation [Ameziani *et al.* 2009].

The effect of thermal fluctuations on the interface velocity in vertical Bridgman configuration was studied numerically by Stelian *et al.* [2002] for a fluid with *Pr=0.07*. The effect of the modulation period on the interface velocity was investigated for a duration ranging between 5 and 3000 s. As a cut-off period for the velocity amplitude was observed it was concluded that temperature oscillations with periods lower than the cut-off one have no harmful effect on the growth process.

Antohe and Lage [1996] investigated the effects of the heating amplitude and frequency on the transport phenomena considering clear fluid and fully saturated porous medium enclosures under time periodic square wave heating in the horizontal direction for a liquid (*Pr=0.71*). It was underlined that the heating amplitude effect is very important since flow resonance appears as the heating frequency matches the natural frequency of the flow sweep inside the enclosure. The resonance frequency was shown to be independent of the heating amplitude for both clear fluid and porous medium configurations.

Voller [1987] developed an accurate method to study this kind of problems based on finite volume approximation and by using the enthalpy porosity formulation

when phase change is involved ($Ste^{-1} \neq 0$). The computational methods developed displayed good agreement in solving transitional flows in the presence of multiple solutions, when compared with finite difference methods coupled with vorticity-stream function formulation [Kaenton 2004] and accurate spectral methods [Achoubir *et al.* 2008].

Semma *et al.* [2005], presented results on the effect of thermovibrational convection in a vertical Bridgman cavity and studied the frequency dependence of the flow intensity and solid/liquid interface deformation acting on the steady and oscillatory basic states. It was shown that with the stationary basic regime, the solid/liquid interface deformation can be affected at low frequencies. However, for high frequencies, the flow and interface deformation converges toward their free constraint state value. In this work, authors neglected the possibility of loss of symmetry which can take place for the strong Rayleigh numbers [Bennacer *et al.* 2006].

For the full cavity, Semma *et al.* [2005], showed the existence of a frequency band for which the initial quasi-periodic regime becomes perfectly periodic. In this case the solid/liquid interface motion and flow in the melt are stabilized. By comparing two situations (with and without phase change), it was noticed that the interaction of the solid/liquid interface with the flow regime cannot be neglected and must be taken into account in a realistic study of directional solidification, especially when considering modulation of heating conditions.

Many studies also focused on the classical rectangular cavity without phase change. The fundamental problem of Kaenton *et al.* [2004] without solutal buoyancy effect ($N = 0$), was extended later by Achoubir *et al.* [2008] to solutal effect ($N \neq 0$).

The double-diffusive convection in a cavity heated from below without modulation has been studied by Achoubir *et al.* [2008]. In steady regimes and for moderate Lewis value ($Le=10$), the flow structure and intensity were generally found to depend strongly on N (N is considered to vary between 0 and 100). For $N = 1$, the transition to oscillatory mode was studied as a function of the Lewis number. The authors showed the existence of three distinct behaviours of the critical Rayleigh number. In the first regime ($Le>100$), the critical Rayleigh number approaches an asymptotic constant value. In the second regime (for intermediate values of Le, $4<Le<100$), the evolution of the critical Rayleigh number can be correlated by the relationship $Ra_C \times Le^{-1/2} \approx 1$. In the third regime ($Le<4$), where the scales for mass and energy diffusion are of the same order; a complex scenario caused by the strong competition between the solutal and the thermal forces is observed.

In the current work modulation is applied in the presence of thermosolutal convection ($N \neq 0$). We consider the effects of the frequency of an imposed thermal oscillation on the hot wall in a cavity heated from below and filled with a binary

fluid at low *Pr* (*Pr=0.01*). Results are compared to available accurate solutions in the situation without temperature modulation. In order to extend our previous study it is chosen to consider first a flat interface moving with a constant velocity and to focus on the effect of thermosolutal interaction with modulation, then the effect of pulling velocity has been considered.

3   Model and validations

The domain under analysis presented in Fig. 1 is a two-dimensional enclosure filled with a viscous, incompressible and Newtonian binary fluid. As shown, the cavity has imposed thermal and solutal vertical gradients. It consists of a square cavity heated from below and cooled from the top by maintaining the respective temperatures T'_H and T'_C of these surfaces constant. The horizontal walls are maintained at constant concentrations: C'_0 (at the top) and C'_1 (at the bottom). The governing equations are solved for the unsteady regime with assumptions of no heat generation, viscous dissipation or thermal radiation. The Soret and Dufour effects are neglected. On thermal boundary layer, an important thermal gradient could induce a non negligible Soret effect and a flow modification occurs [Mahidjiba *et al.* 2003].
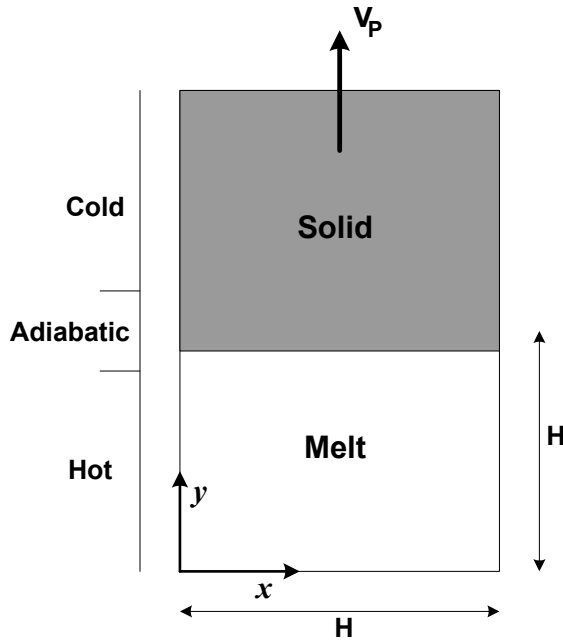

Figure 1: Sketch of the investigated growth configuration

All thermo-physical properties of the fluid are taken constant except for the density variation in the buoyancy term (Boussinesq approximation).

The resulting continuity, momentum, energy and mass coupled equations can be written in dimensionless form as follows:

Continuity equation

$$\frac{\partial u}{\partial x} + \frac{\partial v}{\partial y} = 0 \tag{1}$$

Horizontal velocity component

$$\frac{\partial u}{\partial t} + u\frac{\partial u}{\partial x} + v\frac{\partial u}{\partial y} = -\frac{\partial p}{\partial x} + \Pr \nabla^2 u \tag{2}$$

Vertical velocity component

$$\frac{\partial v}{\partial t} + u\frac{\partial v}{\partial x} + v\frac{\partial v}{\partial y} = -\frac{\partial p}{\partial x} + \Pr \nabla^2 v + Ra_T \Pr(T - NC) \tag{3}$$

Energy equation

$$\frac{\partial T}{\partial t} + u\frac{\partial T}{\partial x} + v\frac{\partial T}{\partial y} = \nabla^2 T \tag{4}$$

Species equation

$$\frac{\partial C}{\partial t} + u\frac{\partial C}{\partial x} + v\frac{\partial C}{\partial y} = \frac{1}{Le}\nabla^2 C \tag{5}$$

In the above equations, the lenghts are reduced by using the height of the cavity H, times by H^2/α leading to the reference velocity α/H, temperature by $\Delta T = T'_H - T'_C$ and concentration by $\Delta C = C'_0 - C'_1$.

The boundary conditions written in the dimensionless form read:

Thermal field $T = 1 + \sin(2\pi ft)$ at $y = 0$; $x = 0, 1$ and $y \in [0 , 0.75]$

$T = 0$ at $y = 1$ $\hfill (6)$

$\frac{\partial T}{\partial x} = 0$ at $x = 0, 1$ and $y \in [0.75, 1]$

Solutal field

$$\frac{\partial C}{\partial y} = V_p \times Le \times (C - 1), \; u = 0, \; v = V_p \text{ for } x = 1$$

$$\frac{\partial C}{\partial y} = V_p \times Le \times (k-1)C, \; u = 0, \; v = V_p \text{ for } x = 0 \tag{7}$$

$\frac{\partial C}{\partial x} = 0, \; u = 0, \; v = V_p \text{ at } x = 0, 1$

The problem is governed by four dimensionless numbers, Thermal Rayleigh Ra_T,Prandtl *Pr*, Lewis *Le* numbers, Peclet number $Pe = V_p$, and the buoyancy ratio N defined positive ($N > 0$) when thermal and solutal buoyancy forces act in the opposite direction.

The Nusselt and Sherwood numbers characterizing, respectively, the non dimensional heat and mass transfer are respectively:

$$Nu = \int_{x=0}^{x=1} \left.\frac{\partial T}{\partial y}\right|_{y=1} dx, \quad Sh = \int_{x=0}^{x=1} \left.\frac{\partial C}{\partial y}\right|_{y=1} dx \tag{8}$$

A variety of methods can be used in principle to solve the equations above (see, e.g., Alami et al. [2009], Bucchignani [2009], Djebali et al. [2009], Mezrhab and Naji [2009] and references in all these works).

Here, a finite volume method has been used (Patankar, 1980). The conductive terms have been discretized with a central differences scheme and the convective terms by using a third order QUICK scheme subjected to a flux limiter (Leonard [1979, 1991]). To resolve the velocity - pressure coupling, the SIMPLEC algorithm has been used (Van Doormal and Raithby [1984]). The temporal discretization is done by using a second order Euler scheme. Extensive validation of the present code performances with and without phase change has been done elsewhere by Semma *et al.* 2005.

A grid sensitivity study was carried out and showed that spatial resolution 64×64 and time step $\Delta t = 5 \times 10^{-4}$ allow an accurate description of the thermosolutal convection phenomena within the cavity.

The numerical method has been also validated by comparison to Bergman and Hyun [1996] results. The configuration considered is a square cavity laterally heated. The left and right walls are respectively maintained at uniform concentrations ($C' = 1$, rich in Sn) and ($C' = 0$, rich in Pb). These authors carried out simulations based on a spectral method and obtained solutions of high accuracy in a broad range of thermal and solutal Rayleigh numbers. We consider here for comparison the case corresponding to $Ra_T = 100$ and $N = -10$. Initially, because of the high thermal diffusion speed process (*Le=7500*), the thermal buoyancy forces settle and give rise to a one convective cell occupying the whole of the domain. In the same way, two boundary solutal layers are developed near the vertical walls resulting in secondary cells turning in the opposite direction. These cells grow with

time reducing the size of the thermal cell. This can be also illustrated by the important decrease of the stream function (table 1). Calculations show good agreement with the reference results.

Table 1: Comparison between Bergman and Hyun calculations (1996) and current results (underlined) for ($Ra_T = 100$ and $N = 10$)

	ψ_{min}	ψ_{max}
t=0.3	ψ_{min}=-0.189, ψ_{min}=-0.182	ψ_{max}=4.94, ψ_{max}=5.00
t=0.13	ψ_{min}=0.0, ψ_{min}=-0.0006	ψ_{max}=0.321, ψ_{max}=0.339

4   Results and discussion

In order to study the effect of the hot wall temperature oscillations on the heat and species transfer and phase change characteristics, the following quantities are commonly used (Kwak *et al.* [1998], Semma et al, [2005]).

$$G(\phi) = \frac{\overline{\phi}(\varepsilon, f)}{\overline{\phi}(0,0)}$$

$$A(\phi) = \frac{\phi_{\max}(\varepsilon, f) - \phi_{\min}(\varepsilon, f)}{\overline{\phi}(0,0)}$$

where, ϕ stands for an arbitrary physical variable and $\bar{\phi}$ is its average value.

The solutal boundary conditions applied to the square cavity have been chosen close to those of real system. The solutal buoyancy force acts in the opposite direction to the thermal buoyancy force.

The full transient Navier–Stokes equations, coupled to energy and species conservation equations, have been solved numerically using the finite volumes technique (it has been assumed that the solid-liquid interface always remains planar and perpendicular to the growth direction; its motion is characterized by a constant Peclet number).

Before presenting the unsteady flow and thermal fields, the behaviour of the steady velocity and temperature fields [Achoubir *et al.* 2008] are briefly described ($\varepsilon = 0$). The streamlines, temperature and concentration contours corresponding to the steady cases with $Ra = 10^4$, $Pe=0.1$ and for high and low values of $N(N = 1$ and $N = 50$) are shown in Fig. 2, illustrating the interaction of the complex flow with the thermal and solutal fields.

For $N = 1$, and because of the boundary conditions and since the non stabilizing thermal gradient is higher than the stabilizing solutal gradient, the thermal forces
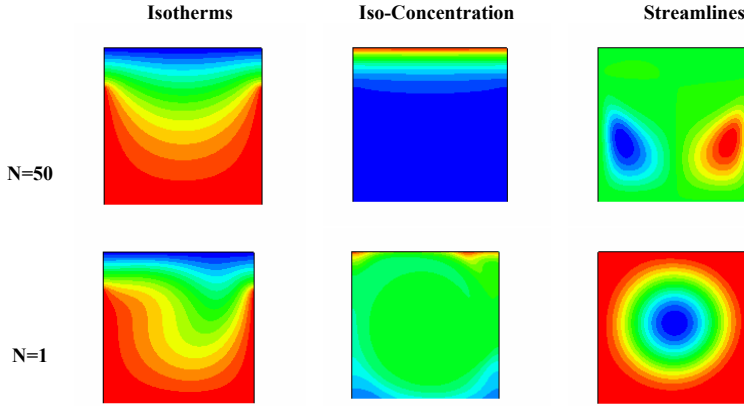
Figure 2: Thermal, solutal and dynamic fields for N=1 and N=50, $Ra_T=10^4$

dominate solutal ones and the flow is controlled completely by the thermal convection (low N). The flow structure is characterized by the predominance of one flow cell (figure 2). As N becomes larger, the solutal force dominates the thermal ones tending to stabilize the system. The flow structure is characterized by two cells rotating in the opposite directions.

Concerning the case of an oscillating temperature (at hot wall, $\varepsilon \neq 0$), the stationary modulated solution corresponding to $Ra=10^4$ and $1.5\mathrm{x}10^4$ is taken as basic states. This solution is convective with a monocellular flow for low N ($N = 0$ and $N = 1$) and diffusive with symmetrical bicellular structure for $N = 50$.

The modulation effects on heat transfer and fluid flow have been studied by varying the nondimensional amplitudes from 0 to 1 and the nondimensional frequencies from 0 to 100.

Starting with the steady state for fixed Ra and N, the oscillating heating temperature was imposed at $t = 0$. In response to the imposed thermal boundary condition, the flow, thermal and solutal fields undergo a transient adjustment period. After certain time duration, the fluid flow and thermosolutal fields reach their respective periodic/aperiodic states. This transitory regime varies according to the variable ϕ and depends on the modulation frequency. We are interested particularly here in the characterization of the established regime.

For $N = O(1)$, we note the predominance of the thermal convection with only one cell. Figure 3 shows $G(\psi_{\max})$ versus the frequency for $Ra=10^4$ and $\varepsilon=1$. For high frequencies ($f > 30$), the modulation does not produce significant effects on the flow intensity and heat/mass transfer in the cavity. This can be explained according to the low value of the Prandtl number (indicating a weak coupling between
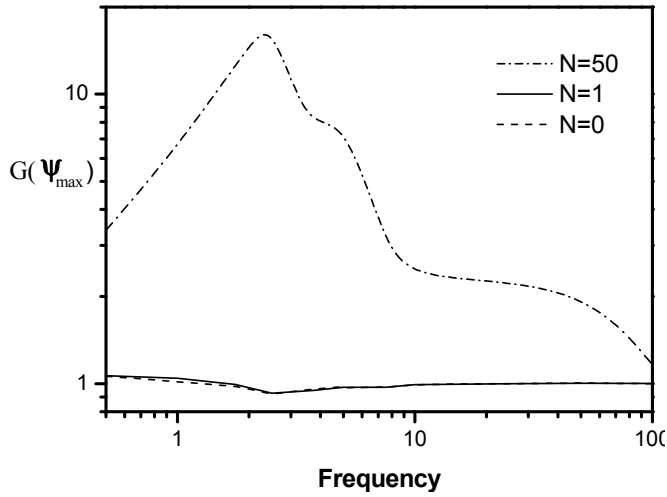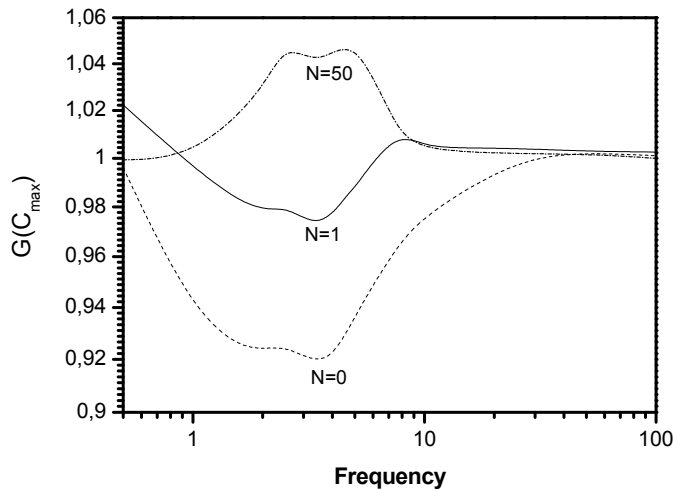
Figure 3: Effect of the thermal modulation on flow intensity

Figure 4: Effect of thermal modulation on C_{max}

the thermal and velocity fields), which provides a reasonable justification for the response of the system to the abrupt temperature change.

For low frequencies, we note the presence of a critical f_c for which ψ_{max} reaches a minimal value. This frequency which is independent on the modulation amplitude is one of the characteristics of the regime. The maximum value of the concentration on the cold wall also falls and reaches a minimal value for the same frequency.
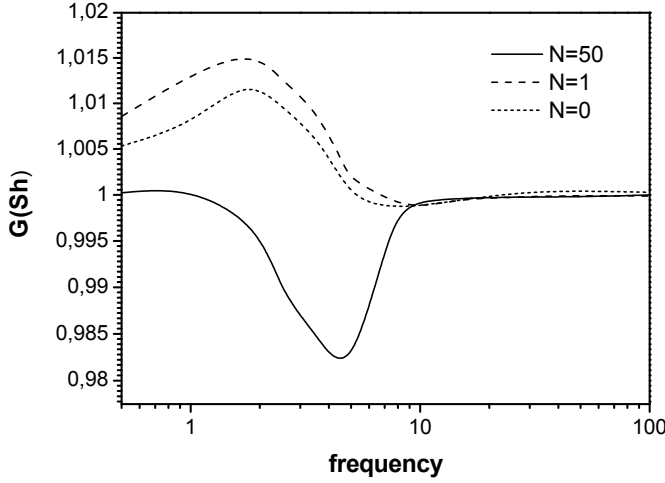
Figure 5: Effect of the thermal modulation on the Sherwood number

This relative value increases with N and passes from 0.92 (for $N = 0$) to 0.97 (for $N = 1$), which shows a sensitivity of this parameter on the ratio of thermal and solutal buoyancy forces (figure 4). The same remark is valid for the variation of the Sherwood number whose relative value increases with the reduction in ψ_{max} value (figure 5).

For $N = 50$, the flow structure is characterized by two symmetrical cells. Indeed, the value of N indicates the predominance of the solutal volume forces, which justifies this transition from only one cell to two symmetrical cells of low intensity. The application of thermal modulation on the hot wall increases the intensity of the flow within the cavity. This increase exceeding 10 times the basic value is quite evident for a critical frequency ($f_C \approx 2.3$). For this frequency, the oscillation amplitude of C_{max} reaches its maximal value (figure 6).

However, this can be observed clearly for $Ra=15000$ (figure 7). For $f = 1.5$ or $f = 2$ (figure 7), the maximum amplitudes are observed for $2f$ and not for f with the presence of other peaks indicating an aperiodic behavior of the system, whereas for the low frequencies ($f = 0.5$) or high frequencies ($f = 20$), the regime is periodic. Increase in Ra leads to a weak increase in the value of $G(\psi_{max})$, but the total behaviour of the evolution of different fields remains practically the same. In figure 8, we present the evolution of C_{max} with flow structures and solutal fields corresponding to four instants of the period. It is noted that when the flow intensity is important, the transport of the solute becomes significant, which however decreases the value of C_{max} at the interface (cold wall). When the flow intensity
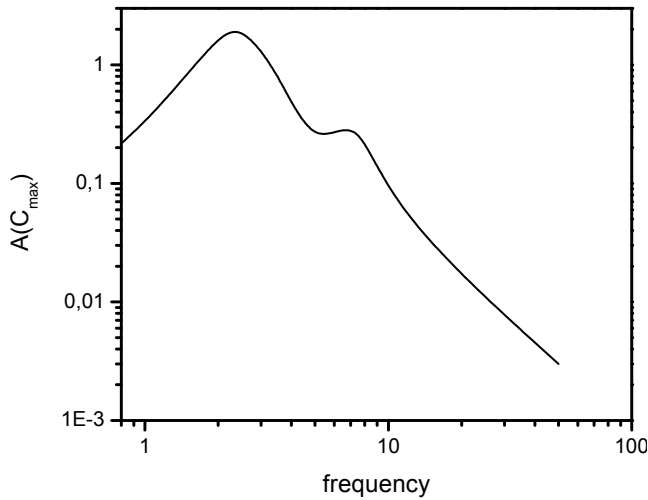
Figure 6: Effect of the thermal modulation on the oscillation amplitude of C_{max}

decreases, the transfer becomes practically purely diffusive with the stratification of concentration near the cold wall and the increase consequently in the value of C_{max}. This is well illustrated in figure 9 where the extrema of ψ_{max} and C_{max} vary in opposite directions.

The effect of the pulling rate was also investigated. This parameter constitutes a significant means for the control of the flow stability in crystal growth configurations.

In their paper, Achoubir *et al.* [2008] studied the effect of the pulling rate on the flow structures. They showed the presence of critical Peclet separating two different modes: for Pe>Pec, solutal boundary layer being important and for Pe<Pec, the concentration being practically uniform with only the thermal buoyancy forces controlling the flow.

We consider here N=50 and Ra=10^4, the critical Peclet being given by the correlation: $Pe_{\overline{C}}0.051 \times e^{-N/18.5} + 0.0046$ (Achoubir *et al.* [2008]). The critical pulling rate corresponding is about Pe$_c$=0.007. To remain in the zone where the solutale gradient is sufficient, we consider the modulation effect on ψ_{max} for Pe=0.1, 0.05 and 0.01.

Figure 10 presents the evolution of $G(\psi_{max})$ as a function of the frequency for *Ra=10^4* and *ε=1*. As noticed before, $G(\psi_{max})$ reaches its maximum value for a cut-off frequency. For *Pe=0.05*, the maximum value is 120. This value is 10 times larger than that corresponding to *Pe=0.1,* which clearly shows the mitigating effect
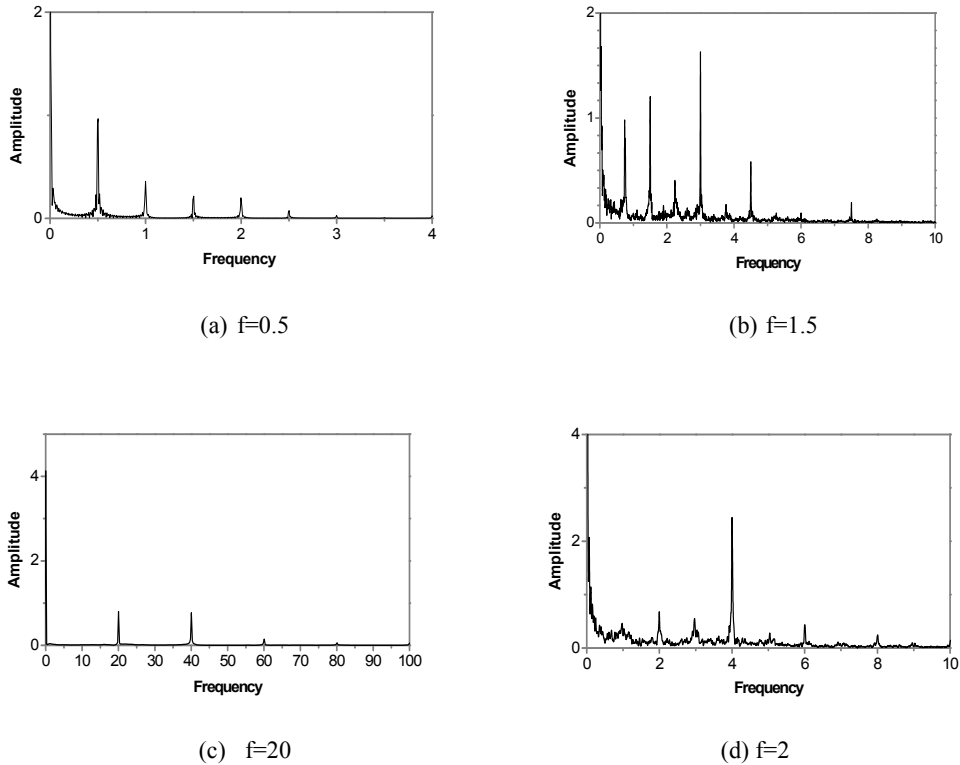
(a) f=0.5

(b) f=1.5

(c) f=20

(d) f=2

Figure 7: Effect of the spectral response of the system for different frequencies and for *Ra=15000* and $N = 50$.

exerted by the Peclet parameter (figure 11).

For Pe=0.01, we note an attenuation on the left and on the right of the cut-off frequency. This can be explained by the weak gradient of concentration that does not allow destabilization of the flow in oscillatory mode.

5 Conclusion

Though important advances on flow visualisation and experimentation have been achieved over recent years, modelling directional solidification should be still regarded as an important way to understand non linear behaviours encountered in crystal growth from the melt. Till date, classically investigated problems have focused on two important control parameters, namely the pulling velocity and the furnace heat profile (and their effect on convective flows and induced transfers inside the domain subject to phase change). In the present work the temperature fluctua-
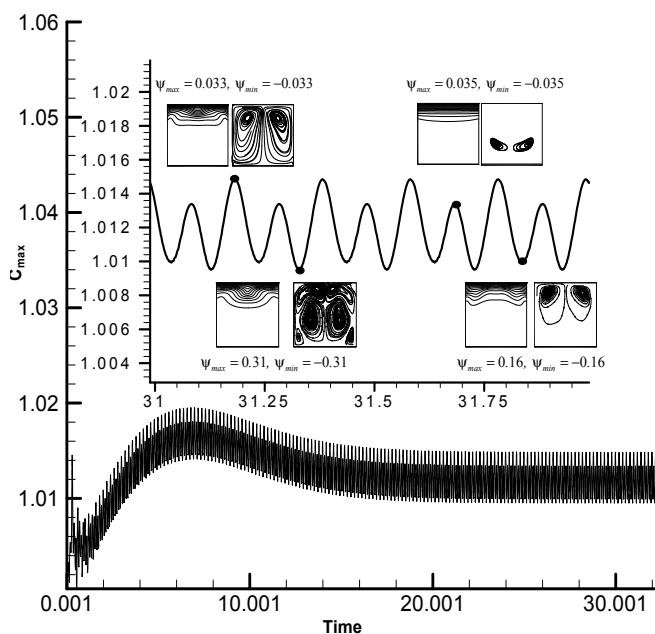
Figure 8: Transient maximal concentration with the flow structures taken in four various half-periods for $Ra=10^4$, $\varepsilon=1$ and $f = 5$.
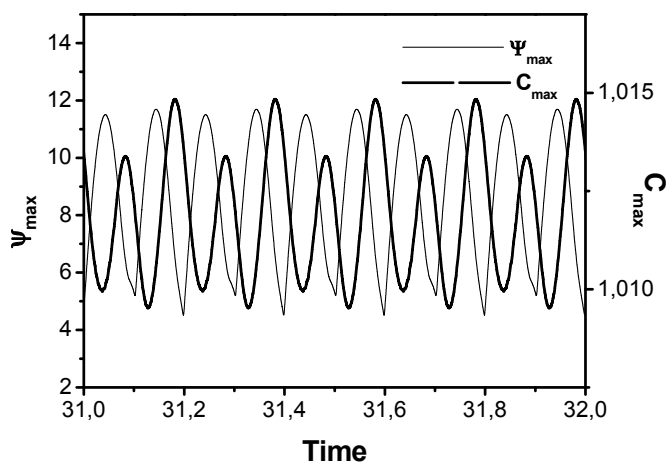

Figure 9: Transient maximal concentration and stream function for $Ra= 10^4$, $\varepsilon=1$ and f=5.
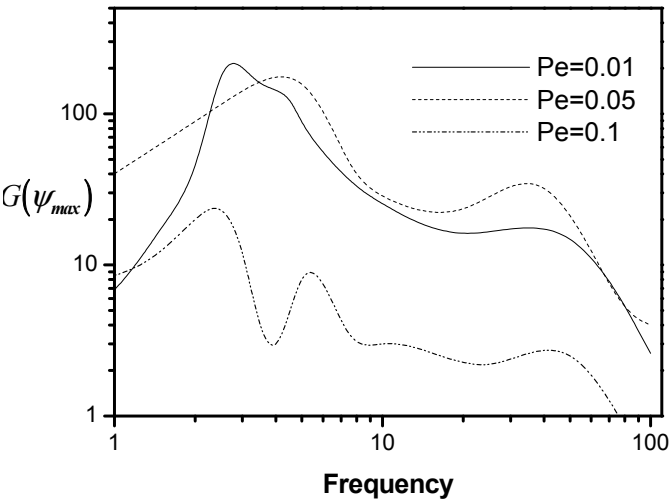
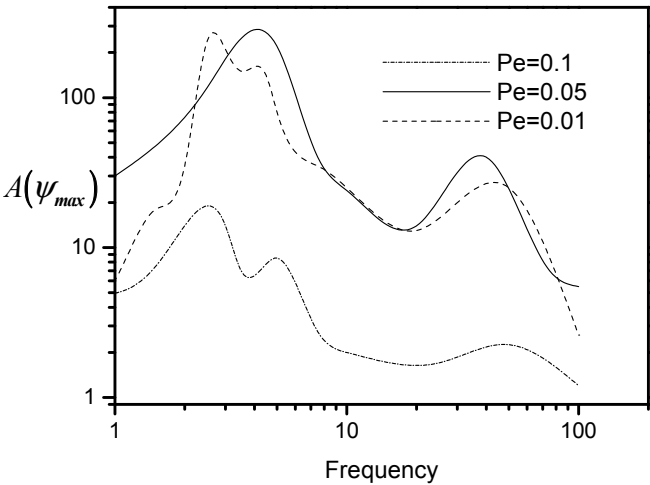Figure 10: Pulling effect on the average value of stream function

Figure 11: Pulling effect on the oscillation amplitude of stream function

tion has been added as an external process-controlling parameter and its effect have been considered not only on the thermal field but also on the solutal one.

The results show the presence of multiple solutions as responses to simultaneous vertical temperature and species concentration gradients. For low values of *N*, the flow intensity is reduced and reaches a minimal value for a critical frequency, whereas for high value of *N* the flow intensity is increased and reaches a maximum value for a threshold frequency slightly lower than the first one. The effect of the pulling rate has been also investigated showing a mitigating action on the modulation when the system is slowly pulled. The present work should be regarded as an additional step towards the understanding of coupled phenomena (consideration of double diffusive convection and modulation).

References

Achoubir K., Bennacer R., Cheddadi A., El Ganaoui M., Semma E. (2008): Numerical Study of Thermosolutal Convection in Enclosures Used for Directional Solidification (Bridgman Cavity), *FDMP: Fluid Dynamics and Materials Processing*, Vol. 4, No. 3, pp. 199-210.

Achoubir K., Semma E., Cheddadi A. (2008): Investigation de l'effet du tirage sur le transfert thermique dans une cavité de Bridgman verticale, *Journal of Phy. and Chim. News*, (in press).

Alami M. E., Semma E., Najam M., and Boutarfa R. (2009): Numerical Study of Convective Heat Transfer in a Horizontal Channel, *FDMP: Fluid Dynamics and Materials Processing.*, Vol. 5, No. 1, pp. 23-36.

Ameziani D.E., Bennacer R., Bouhadef K., Azzi A. (2009): Effect of the days scrolling on the natural convection in an open ended storage, *IJTS*, 1-9 (in press).

Antohe B.V., Lage J.L. (1996): Amplitude effect on convection induced by time periodic horizontal heating,. *Int. J. Heat Mass Transfer*, Vol. 39, pp. 1121-1133.

Bennacer R., EL Ganaoui M., Leonardi E. (2006): Vertical Bridgman Configuration Heated From Below: 3D Bifurcation And Stability Analysis, *Applied Mathematical Modelling*, Vol 30, No. 11, pp. 1249-1261.

Benielli D., El Ganaoui M., Semma E., Bergeon N., Jamgotchian H., Voge P., Billia B., Bontoux P. (2001): Effect of thermal convection on directional solidification of succinonitrile-acetone alloys: Comparison between experimental and numerical studies. *Journal de Physique IV.*, Vol. 11, Pr 6, pp. 135-143.

Bergman T. L., Hyun M. T. (1996): Simulation of two-dimensional thermosolutal convection in liquid metals induced by horizontal temperature and species gradients, *Int. J. Heat Mass Transfer*, Vol. 39, No. 14, pp. 2883-2894.

Bucchignani E. (2009): An Implicit Unsteady Finite Volume Formulation for Natural Convection in a Square Cavity, *FDMP: Fluid Dynamics and Materials Processing*., Vol. 5, No. 1, pp. 37-60.

Crespo del Arco, E., Pulicani, J.P., Bontoux, P. (1989): Simulations and analysis of time-dependent convection in low Pr fluids, *Int J. Phys. Chem. Hydrodyn*, Vol. 11, No. 6, pp. 681-692.

Djebali R., El Ganaoui M., Sammouda H., Bennacer R. (2009): Some Benchmarks of a Side Wall Heated Cavity Using Lattice Boltzmann Approach, *FDMP: Fluid Dynamics and Materials Processing*, Vol. 5, No. 3, pp. 261-282.

El Ganaoui M. (2002): Computational modelling of heat mass and solute transport in solid/liquid transition systems on earth and on microgravity environment. MECOM 2002, Santa Fe, Argentina, 28-31 0ctobre 2002. *Mecanica Computational*, vol XXI, ISSN 1666-6070, Eds. S. R. Idelsohn, V. Sonzogi, A. Cardona, pp. 2587-2592.

El Ganaoui, M., Bontoux P. (1998): An Homogenisation Method for Solid-Liquid Phase Change During Directional Solidification, ASME H.T.D., *Num. and Engineering Methods in Heat Transfer*, Vol. 361, pp. 453-469.

El Ganaoui M., Bontoux P., Morvan D. (1999): Localisation d'un front de solidification en interaction avec un bain fondu instationnaire. - C. R. Acad. Sci. Paris, série IIb, t. 327, pp. 41-48.

El Ganaoui M., Prud'homme R., Bennacer R. (2007): Melting and solidification : processes and models, *Comptes Rendus Mécanique*, Vol. 335, No. 5-6.

Kaenton J., Semma A., Timchenko V., El Ganaoui M., Leonardi E., de Vahl Davis G. (2004): Effects of anisotropy and solid/liquid thermal conductivity ratio on flow instabilities during inverted Bridgman growth, *Int. J. Heat and Mass Transfer*, Vol. 47, pp. 3403-3413.

Larroudé P., Ouazzani. J., Alexander. J. I. D., Bontoux. P. (1994): Symmetry breaking transition and oscillatory flows in a 2D directional solidification model, *Eur. J. Mech, B/Fluids*, Vol. 13, pp. 353-381.

Mahidjiba A., Bennacer R., Vasseur P. (2003): Effect Of The Boundary Conditions On Convection In A Horizontal Fluide Layer With The Soret Contribution, *Acta Mechanica*, Vol. 160, No. 3-4, pp. 161-177.

Mezrhab A., Naji H. (2009): Oupling of Lattice Boltzmann Equation and Finite Volume Method to Simulate Heat Transfer in a Square Cavity, *FDMP: Fluid Dynamics and Materials Processing*., Vol. 5, No. 3, pp. 283-296.

Patankar S.V. (1980): *Numerical heat transfer and fluid flow*, McGraw-Hill.

Prud'homme R., El Ganaoui M. (2006): Solid/Liquid Phase Change: Recent

Studies and Models, *FDMP: Fluid Dynamics and Materials Processing*, Vol.2, No. 1, pp.11-21.

Pulicani J. P., Crespo Del Arcoe E., Randriamampianina A., Bontoux P., Peyret R. (1990): Spectral simulation of oscillatory convection at low Pr, *Int J Num Meth Fluids*, Vol. 10, pp. 481-517.

Semma A., El Ganaoui M., Cheddadi A., Bontoux P. (2003): Instability of melt flow and solidification front during horizontal growth. *Comptes Rendus de l'Académie des Sciences (Mécanique)*, Vol. 331, pp. 631-639.

Semma E. A., El Ganaoui M., Timchenko V., Leonardi E. (2005): Some Thermal Modulation Effects on Directional Solidification, *FDMP: Fluid Dynamics and Materials Processing*., Vol. 2, No. 3, pp. 191-202.

Semma E. A.; El Ganaoui M.; Timchenko V.; and Leonardi E. (2006): Thermal Boundary modulation fluid effect on the flow and conctration field agjacent to the solid/liquid interface, *Annals of the Assembly for International Heat Transfer Conference 13*.

Stelian C., Duffar T., Santailler J.-L., Nicoara, I. (2002): Influence of temperature oscillations on the interface velocity during Bridgman crystal growth, *Journal of Crystal growth,* Vols. 237-239, pp. 1701-1706.

Van Doormal J.P., Raithby G.D. (1984): Enhancements of the SIMPLE method for predicting incompressible fluid flows, *Num. Heat Transfer*, Vol. 7, pp. 147-163.

Voller, Prakash (1987): A fixed grid numerical modelling methodology for convection diffusion mushy region phase change problems, *Int. Heat Mass transfer* Vol. 30, pp. 1709-1719.